A Quantum Computational Approach to Correspondence Problems on Point Sets
— Supplementary Material —

Vladislav Golyanik Christian Theobalt
Max Planck Institute for Informatics, Saarland Informatics Campus

In this document, we provide additional details on the selection of the annealing rate, analyse the structure of $\mathbf{P}$ and formalise the unembedding, *i.e.,* the conversion of the solution to QUBOP (16) to the solution of the original alignment problem on point sets. We preserve the notations referring to the sections and equations from the main matter. The equations and the figure introduced in this supplement are equipped with Roman numerals.

Annealing Rate

Suppose $E_n(s)$ is the ground state of instantaneous Hamiltonian, $E_n(0)$ is the initial state (ground state) of the system and $E_m(s)$ is any other excited state of the instantaneous Hamiltonian. Let $s = \frac{t}{T} \in [0; 1]$, where T is the overall time of interpolation and t is physical time. Then, according to [1], T has to be chosen so that

$$T \gg \frac{|\langle E_m(s)|dH/ds|E_n(s)\rangle|}{E_{nm}(s)^2}, \ \forall m \neq n, \qquad \text{(i)}$$

where dH/ds is the rate of change of Hamiltonian with respect to s and E_{nm} is the difference in the corresponding instantaneous energies.

Analysis of $\mathbf{P}$

Fig. I visualises several exemplary weight matrices $\mathbf{P}$ from the experiments with clean and noisy data (see Sec. 7). There are several observations. First, $\mathbf{P} = \mathbf{\Phi}\mathbf{\Phi}^\mathsf{T}$ is symmetric upon algorithm design. We also see that the columns of $\mathbf{\Phi}$ can be arbitrarily reshuffled as long as the correspondences are preserved[1]. Second, $\mathbf{P}$ contains regularly arranged zero submatrices, due to our choice of the basis. As soon as a row of $\mathbf{\Phi}$ induced by $q\mathbf{C_I}$, where $\mathbf{C_I} \in \{\mathbf{I}, -\mathbf{I}\}$, is multiplied by a column of $\mathbf{\Phi}^\mathsf{T}$ induced by $q\mathbf{C_M}$, where $\mathbf{C_M} \in \{\mathbf{M}, -\mathbf{M}\}$, and vice versa, we obtain a zero entry

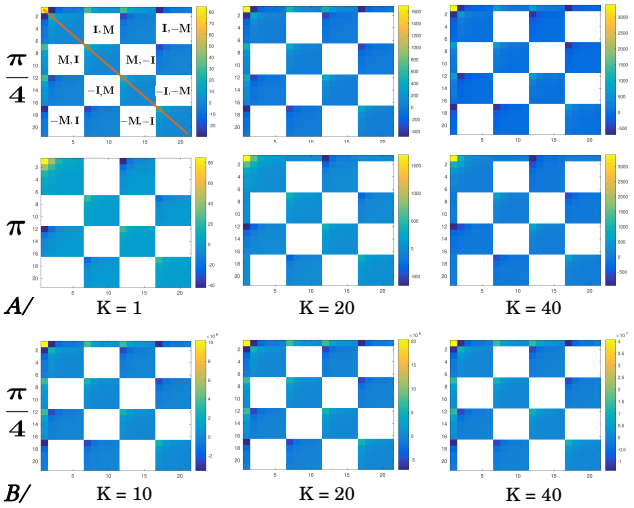

Figure I: Exemplary visualisations of the weight matrix $\mathbf{P} = \mathbf{\Phi}\mathbf{\Phi}^\mathsf{T}$ in the experiment with clean (***A/***) and noisy data with 35% of outliers in the template (***B/***), for $K \in \{1, 10, 20, 40\}$ and $\theta \in \{\frac{\pi}{4}, \pi\}$. The colour scheme and the range of energy values are given to the right of each $\mathbf{P}$. White colour stands for zero entries. The diagonal values in $\mathbf{P}$ represent biases (marked in orange on the top left), and non-zero elements represent couplings between the qubits. In the visualisation on the top left, we list the pairs of $\mathbf{C} \in \{\mathbf{I}, \mathbf{M}, -\mathbf{I}, -\mathbf{M}\}$ eventually leading to zero matrices.

in $\mathbf{P}$. The reason is that

$$\begin{cases} [\mathbf{I} \sum_i \mathbf{y}_i]^\mathsf{T} & [\mathbf{M} \sum_j \mathbf{y}_j] & = 0 \\ [-\mathbf{I} \sum_i \mathbf{y}_i]^\mathsf{T} & [\mathbf{M} \sum_j \mathbf{y}_j] & = 0 \\ [\mathbf{I} \sum_i \mathbf{y}_i]^\mathsf{T} & [-\mathbf{M} \sum_j \mathbf{y}_j] & = 0 \\ [-\mathbf{I} \sum_i \mathbf{y}_i]^\mathsf{T} & [-\mathbf{M} \sum_j \mathbf{y}_j] & = 0 \end{cases}, \qquad \text{(ii)}$$

if $\sum_i \mathbf{y}_i = \sum_j \mathbf{y}_j$, which holds in our case since each row of $\mathbf{\Phi}$ except the first row includes all points of $\mathbf{Y}$ multiplied by a single basis element $\mathbf{Q}_k$ (see Fig. I-(top left) for $\mathbf{C}$ pairs resulting in zero matrices). Third, the structure of $\mathbf{P}$ reflects that its diagonal entries encode biases, and non-diagonal elements represent couplings between the qubits.

With the increasing K, the span of the absolute energy values increases, due to the higher number of point interactions. As expected, $\mathbf{P}$ depends on data and the angle of initial misalignment between the point sets. For all possi-

[1] a reshuffling of rows requires changing the order of elements in $\mathbf{Q}$

ble inputs and initial conditions — point sets of different cardinalities, K and θ — the structure of $\mathbf{P}$ is the same for the chosen basis. From $\mathbf{P}$, we also recognise that the considered alignment problem is not purely combinatorial and requires high-precision weights $J_{j,k}$ in (5).

Unembedding

Unembedding is the decoding of the solution to QUBOP (16) to the solution of the original alignment problem. Upon the design, our QA method assembles the entries of the transformation matrix in the additive basis $\mathbf{Q}_k$ (see Secs. (5.1)–(6.1)). Suppose $\hat{\mathbf{q}}$ is the measurement result of $\mathbf{q}$, *i.e.,* it is a classical bitstring with $K+1$ elements. Recall that $\mathbf{q}_1$ is reserved for reference points and does not contribute to the assembly of the transformation. Once $\hat{\mathbf{q}}$ is measured and returned, we obtain the corresponding transformation $\mathbf{R}$ by summing up $\mathbf{Q}_k$ multiplied by $\hat{\mathbf{q}}_{k+1}$:

$$\mathbf{R} = \sum_k \hat{\mathbf{q}}_{k+1} \mathbf{Q}_k. \tag{iii}$$

The obtained $\mathbf{R}$ is an affine transformation. If the solution has to represent a valid rotation matrix $\mathbf{R}_\mathrm{r}$, $\mathbf{R}$ can be projected to the rotation group by solving the *closest orthogonal approximation problem with constraints*:

$$\begin{aligned} &\min \|\mathbf{R}_\mathrm{r} - \mathbf{R}\|_{\mathcal{HS}}^2 , \\ &\text{s. t. } \mathbf{R}_\mathrm{r}^{-1} = \mathbf{R}_\mathrm{r}^\mathsf{T} \text{ and } \det(\mathbf{R}_\mathrm{r}) = 1. \end{aligned} \tag{iv}$$

For a solution to (iv) by singular value decomposition, see [2].

References

[1] Mohammad H. S. Amin. Consistency of the adiabatic theorem. *Phys. Rev. Lett.*, 102:220401, 2009. 1

[2] Nicholas J. Higham. Matrix nearness problems and applications. *Applications of Matrix Theory*, 22, 1989. 2